

## MODELING AND SIMULATION OF A HYDROCRACKING UNIT

HASSAN A. FARAG<sup>1</sup>, N. S. YOUSEF<sup>2</sup>, RANIA FAROUQ<sup>2,\*</sup>

<sup>1</sup>Chemical Engineering Department, Faculty of Engineering, Alexandria University,  
Alexandria, Egypt

<sup>2</sup>Petrochemical Department, Faculty of Engineering, Pharos University, Canal El  
Mahmoudeya St. Semouha, Alexandria, Egypt

\*Corresponding Author: rania\_farouq29@yahoo.com

### Abstract

Hydrocracking is used in the petroleum industry to convert low quality feed stocks into high valued transportation fuels such as gasoline, diesel, and jet fuel. The aim of the present work is to develop a rigorous steady state two-dimensional mathematical model which includes conservation equations of mass and energy for simulating the operation of a hydrocracking unit. Both the catalyst bed and quench zone have been included in this integrated model. The model equations were numerically solved in both axial and radial directions using Matlab software. The presented model was tested against a real plant data in Egypt. The results indicated that a very good agreement between the model predictions and industrial values have been reported for temperature profiles, concentration profiles, and conversion in both radial and axial directions at the hydrocracking unit. Simulation of the quench zone conversion and temperature profiles in the quench zone was also included and gave a low deviation from the actual ones. In concentration profiles, the percentage deviation in the first reactor was found to be 9.28 % and 9.6% for the second reactor. The effect of several parameters such as: Pellet Heat Transfer Coefficient, Effective Radial Thermal Conductivity, Wall Heat Transfer Coefficient, Effective Radial Diffusivity, and Cooling medium (quench zone) has been included in this study. The variation of Wall Heat Transfer Coefficient, Effective Radial Diffusivity for the near-wall region, gave no remarkable changes in the temperature profiles. On the other hand, even small variations of Effective Radial Thermal Conductivity, affected the simulated temperature profiles significantly, and this effect could not be compensated by the variations of the other parameters of the model.

Keywords: Mathematical model, Two-dimensional model, Simulation, Hydrocracking process, Fixed bed reactor, Quench zone.

**Nomenclatures**

$a$	Specific surface area, $m^{-1}$
$Bi$	Biot number
$C_i$	Concentration of species $i$ , $mol/m^3$
$C_p$	Heat capacity of species $i$ , $kcal/kg\ ^\circ C$
$d_t$	Tube diameter, $m$
$D_e$	Effective radial diffusivity, $m^2/s$
$E$	Activation Energy, $kJ/mol$
$h$	Heat transfer coefficient, $kcal/m^2.s.^{\circ}C$
$k$	Reaction rate constant, $h^{-1}$
$L$	Reactor height, $m$
$LHSV$	Liquid hourly space velocity, $hr^{-1}$
$M$	Molecular Weight, $kg/kmol$
$Nu$	Nusselt Number
$Q$	Heat released or absorbed, $kcal/s$
$Pe$	Peclet Number
$Pr$	Prandtl Number
$R$	Reaction rate per unit volume of catalyst, $kg/m^3.s^{-1}$
$r$	Radius of reactor, $m$
$Re$	Reynolds Number
$S$	Concentration of sulphur
$N$	Concentration of nitrogen
$T$	Absolute temperature, $K$
$u$	Superficial velocity, $m/s$

**Greek symbols**

$\varepsilon$	Void fraction of packed bed
$\lambda_{er}$	Effective radial thermal conductivity, $kcal /m. s. C.$
$\mu$	Fluid viscosity, $kg/(m.s)$
$\rho$	Fluid density, $kg/m^3$
$v_L$	Specific volume of liquid feed stock, $m^3/kg$
$v_{H_2}$	Specific volume of $H_2$ , $m^3/kg$
$v_c^L$	Critical specific volume of liquid feed stock, $m^3/kg$
$v_c^{H_2}$	Critical specific volume of $H_2$ , $m^3/kg$

**Subscripts**

$a$	axial
$b$	bulk
$c$	catalyst
$f$	fluid
$s$	solid
$R$	radial
$w$	wall

**Abbreviations**

HDS	The hydro desulfurization reactions
HDN	The hydro de nitrogenation reactions

## 1. Introduction

Hydrocracking is one of the most versatile of all petroleum-refining processes [1]. It is a catalytic process used in refineries for converting heavy oil fractions into high quality middle distillates and lighter products such as diesel, kerosene, naphtha and LPG. The process takes place in hydrogen-rich atmosphere at high temperatures (260-420 °C) and pressures (35-200 bar). The main hydrocracking reactions are cracking and hydrogenation, which occurs in the presence of a catalyst under specified operating conditions: temperature, pressure, and space velocity [2]. A bi-functional catalyst is used in the process in order to facilitate both the cracking and hydrogenation. The cracking function of the catalyst is provided by supporting it with an acidic support consisting of amorphous oxides and a binder, where as providing the hydrogenation function can be achieved by using metals [3]. The cracking reaction is slightly endothermic while the hydrogenation reaction is highly exothermic. Hence, the overall hydrocracking process is highly exothermic. The feedstock is generally vacuum gas oil (VGO) or heavy vacuum gas oil (HVGO) [4].

A new, even more efficient, approach to obtain high quality middle distillates and lighter products in hydrocracking process is the two-stage uni-cracking process. [5]. Modeling methodologies developed over the years for hydrocracking and can be classified into two categories (1): lumping models and (2) mechanistic models.[6] Many kinetic models for the hydrocracking process have been proposed [7-12]. Earlier studies reported by other researchers focused on the calculation of conversion, and temperature profiles in the axial direction only [13-15], few studies were published for modeling packed bed reactors in both axial and radial direction.[16-18]. This research paper aims to validate the model of the hydrocracking unit in both axial and radial direction. The computer program used in the present study was Matlab which is a high performance language for technical computing and is now considered a standard tool in most universities and industries worldwide [19]. The presented model was tested against real plant data, and the operational conditions of the hydrocracking unit are shown in Table 1.

**Table 1. Industrial data for the hydrocracking reactor.**

Parameter	Value	Unit
Reactor Internal Diameter	4.734	m
Feed flow rate	221.9	m <sup>3</sup> /hr
Inlet pressure	183	bar
Inlet temperature	425	°C
Catalyst bed porosity	0.345 - 0.55	
Bed bulk density	658	kg/m <sup>3</sup>
Particle diameter	2×10 <sup>-3</sup>	m

## 2. Model Development

In the present study a steady state two-dimensional model was developed for a hydrocracking unit taking into account the radial dispersion. The studied hydrocracking unit consists of two multiple fixed bed catalytic reactors in series. Mass and heat transfer in both radial and axial directions was used to describe the concentration and temperature profiles in the hydrocracking unit using parameters

such as: effective radial diffusivity, effective radial heat conductivity, pellet heat transfer coefficient, and wall heat transfer coefficient. The effective heat- and mass transfer parameters are not only a function of the physical properties of the applied catalyst and the fluid phase, but are also determined by the flow conditions, the reactor (tube) size.

## 2.1. Assumptions

For this model we consider a cylindrical packed-bed reactor of diameter  $D$  and height  $L$ ; We make the following assumptions:

- The process is operating in steady state.
- The velocity profile is constant over the tube radius.
- There are no heat losses by radiation.
- Since  $H_2$  is in excess, hydrocracking is a first order pseudo-homogeneous reaction with respect to reacting materials.
- The diffusivity in the axial direction was found to be insignificant compared to the axial convection. Similarly, the thermal conductivity in the axial direction has a negligible magnitude. [20]
- Axial symmetry is assumed, which is allowed if the described reactor is carefully packed to avoid variation of the porosity in angular direction.

## 2.2. Model equations for the fixed bed

The mass balance equation can be written as

$$u \cdot \nabla C_i - \nabla(D_{er} \nabla C_i) = R \quad (1)$$

with boundary conditions:

$$C_i = C_0 \quad \text{at } z = 0 \quad (2)$$

$$\frac{\partial C_i}{\partial r} = 0 \quad \text{at } r = 0 \quad (3)$$

$$\frac{\partial C_i}{\partial r} = -\frac{k}{D_{er}}(C_i - C_{iw}) \quad \text{at } r = R \quad (4)$$

The energy balance equation for the reactor can be written as [21]:

$$\rho \cdot C_p \cdot u \cdot \nabla T - \nabla \cdot (\lambda \nabla T) = Q \quad (5)$$

$$T_i = T_o \quad \text{at } z = 0 \quad (6)$$

$$\frac{\partial T_i}{\partial r} = 0 \quad \text{at } r = 0 \quad (7)$$

$$\frac{\partial T_i}{\partial r} = -\frac{h_w}{\lambda_{er}}(T - T_w) \quad \text{at } r = R \quad (8)$$

### 2.3. Model equations for the quench zone

The mass balance equation can be written as following [22]:

$$D_{ea} \cdot \frac{d^2 C_i}{dz^2} + u \cdot \frac{dC_i}{dz} = k_{H_2}^L \cdot a \cdot (C_{ib} - C_{iw}) \tag{9}$$

$$C_i = C_{\text{exit from previous bed}} \quad \text{at } z = 0 \tag{10}$$

$$\frac{\partial C_i}{\partial z} = 0 \quad \text{at } z = L \tag{11}$$

$$\lambda \cdot \frac{d^2 T}{dz^2} + u \cdot C_p \frac{dT}{dz} = h_{H_2}^L \cdot a \cdot (T_b - T_w) \tag{12}$$

$$T_i = T_{\text{exit from previous bed}} \quad \text{at } z = 0 \tag{13}$$

$$\frac{\partial T}{\partial z} = 0 \quad \text{at } z = L \tag{14}$$

### Reaction Kinetics

Due to the tremendous complexity of heavy petroleum fractions, lumping is used to formulate reaction kinetics for converting units; however the rates of reaction can be described in simple mathematical terms. From kinetic theory, reaction rate is [23]:

$$\frac{dC}{dt} = kC^n \tag{15}$$

From which

$$\int_{C_f}^{C_p} \frac{dC}{C^n} = \int_0^t k dt \tag{16}$$

where  $C$  is the concentration of reactant,  $C_f$  represents the feed concentration,  $C_p$  represents the product concentration,  $k$  is the rate constant,  $n$  is the reaction order and  $t$  is the time. If  $n=1$  (first-order reaction), then

$$k = LHSV \cdot \ln\left(\frac{C_f}{C_p}\right) \tag{17}$$

where LHSV is the liquid hourly space velocity ( $h^{-1}$ ). From empirical rate measurements in laboratory tests, the rate constant is a function of temperature,

$$k = A \cdot e^{-E_A/RT} \tag{18}$$

where  $A$  is the Arrhenius activity coefficient,  $E_A$  is the activation energy,  $R$  is the universal gas constant and  $T$  is the temperature (absolute).

It is generally accepted that hydrocracking reactions can be adequately modelled by first-order kinetics with respect to the concentration of hydrocarbon feedstock. [9]

The first-order rate expressions employed for typical hydrocracking reactions are the following:

$$k_{HDS} = LHSV \cdot \ln\left(\frac{S_f}{S_p}\right) \quad (19)$$

$$k_{HDN} = LHSV \cdot \ln\left(\frac{N_f}{N_p}\right) \quad (20)$$

A list of correlations for determining oil properties at the process conditions, and mass-transfer coefficients at the gas–liquid and liquid–solid interfaces that are used in the model equations is given in Table 2.

**Table 2. Correlations used in the model equations.**

Parameter	Correlation
<b>Oil density[24]</b>	$\rho_L = \rho_o + \Delta\rho_P - \Delta\rho_T$ $\Delta\rho_P = [0.167 + 16.181 * 10^{-0.0425\rho_o}] \left[\frac{P}{1000}\right]$ $- 0.01 * [0.299 + 263 * 10^{-0.0603\rho_o}] \left[\frac{P}{1000}\right]^2$ $\Delta\rho_T = \left(0.0133 + 152.4(\rho_o + \Delta\rho_P)^{-2.45}\right) [T - 520]$ $- [8.1 * 10^{-6} - 0.0622 * 10^{-0.764(\rho_o + \Delta\rho_P)}] [T - 520]^2$
<b>Dynamic oil viscosity[24]</b>	$\mu_L = 3.141 * 10^{10} (T - 460)^{-3.444} [\log_{10}(API)]^a$ $a = 10.313 [\log_{10}(T - 460)] - 36.447$
<b>Molecular diffusivity[24]</b>	$D_{H_2}^L = 8.93 * 10^{-8} \frac{v_L^{0.267} T}{v_{H_2}^{0.433} \mu_L}$ <p>Where :</p> $v_L = 0.285(v_C^L)^{1.048}$ $v_{H_2} = 0.285(v_C^{H_2})^{1.048}$
<b>Gas–liquid mass transfer coefficient[24]</b>	$\frac{K_{H_2}^L a_L}{D_{H_2}^L} = 7 \left(\frac{G_L}{\mu_L}\right)^{0.4} \left(\frac{\mu_L}{\rho_L D_{H_2}^L}\right)^{0.5}$
<b>Gas–liquid heat transfer coefficient[25]</b>	$Nu_{TP} = 0.5 \left(\frac{\mu_G}{\mu_L}\right)^{1/4} Re_{TP}^{0.7} Pr_L^{1/3} \left(\frac{\mu_B}{\mu_W}\right)^{0.14}$

### 3. Results and Discussion

The model discussed in the present work consists of a set of partial differential equations and linear equations which need to be handled with precise methods of calculations. The model presented is solved with MATLAB software which is a tool for solving numerical mathematical – both linear equations and differential equations.

### 3.1. Effect of pellet heat transfer coefficient ( $h_p$ ) on temperature profile

Handley and Hegg's Correlation, and Wakao et al. Correlation [26] shown in Table 3 which are used for evaluating the pellet heat Transfer Coefficient ( $h_p$ ) were tested. It was found that the correlation of Wakao et al. [26] gave the highest heat transfer coefficient which accordingly raised the amount of heat generated and increased the temperature values in such a way that make it closer to the measured values. The chosen correlation gave a temperature increase across the bed of about 7 °C. Figure 1 shows the temperature profile in the axial direction using Handley and Hegg's, and Wakao et al. It is clear from Fig. 1 that Wakao et al. correlation predicts the reactor temperature profile with a higher accuracy than Handley and Hegg's.

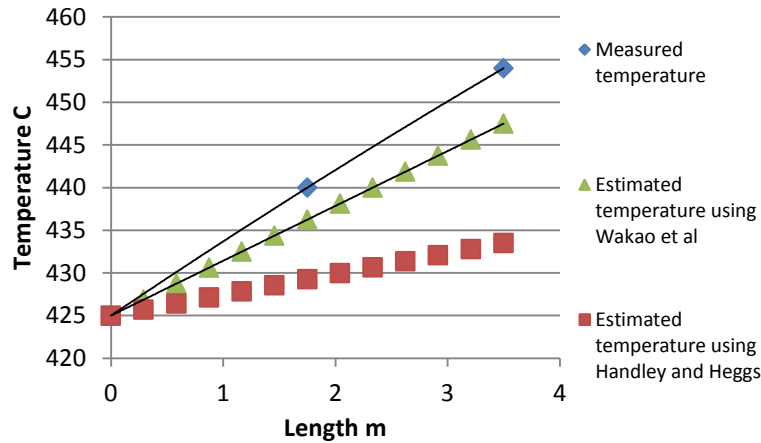
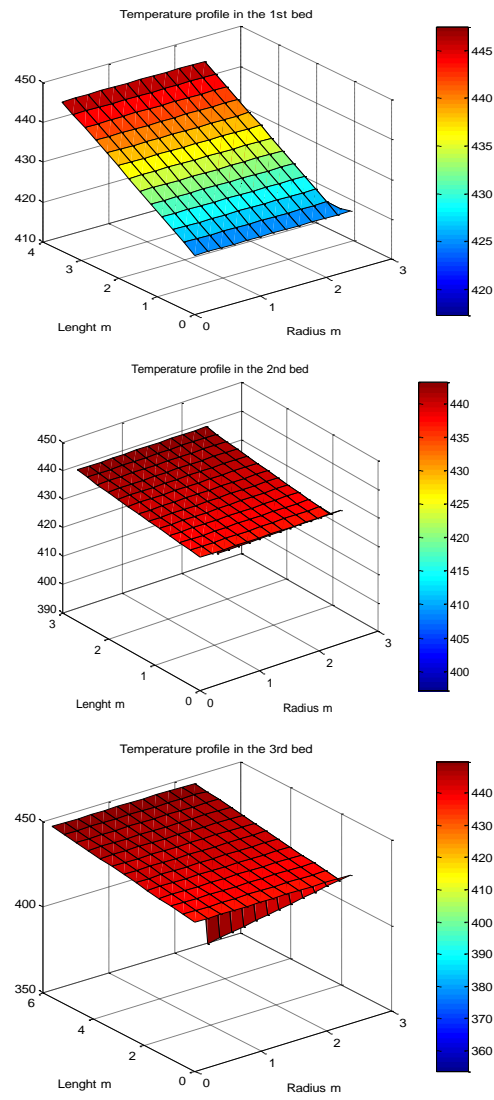


Fig. 1. Actual and estimated temperature profile in the axial direction using different correlations for calculating  $h_p$ .

Table 3. Experimental correlations for the pellet heat transfer coefficient ( $h_p$ )

Authors	Pellet Heat Transfer Coefficient ( $h_p$ )
Handley and Hegg's[24]	$Nu_{fs} = 0.255 \cdot Pr^{1/3} Re_p^{2/3}$
Wakao et al. [24]	$\frac{h_s d_p}{k_g} = 2 + 1.1 Pr^{1/3} (Re)_p^{0.6}$

A three dimensional temperature profile in the first and second reactor are shown in Figs. 2 and 3 respectively.



**Fig .2. Three dimensional Temperature profile in the first reactor (first, second and third beds).**



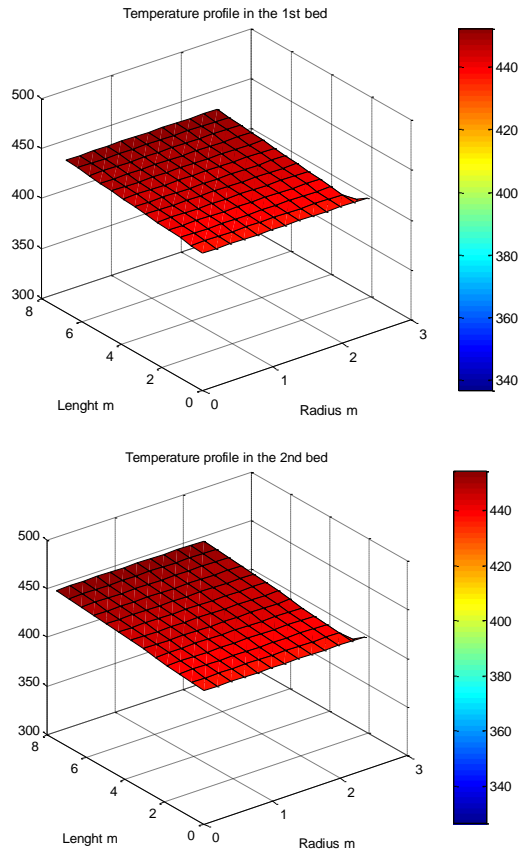


**Fig. 3. Three dimensional temperature profile in the second reactor (first and second beds).**

**3.2. Effect of effective radial thermal conductivity ( $\lambda_{er}$ ) on temperature profile**

Many correlations were tested in order to calculate the value of the effective radial thermal conductivity that can give a temperature profile close to the actual one. However, only two correlations Brunell et al. [27] and Dwmirel et al. [27] shown in table 4, gave suitable values for the effective thermal conductivity in both axial and radial directions as shown in Figs.4 and 5 respectively.

**Table 4. Experimental correlations for effective radial thermal conductivity.**

Author	Effective radial thermal conductivity
Brunell et al. [27]	$\frac{k_{er}}{k_f} = 5.0 + 0.061 Re_p$
Dwmirel et al. [27]	$\frac{k_{er}}{k_f} = 2.894 + 0.068 Re_p$

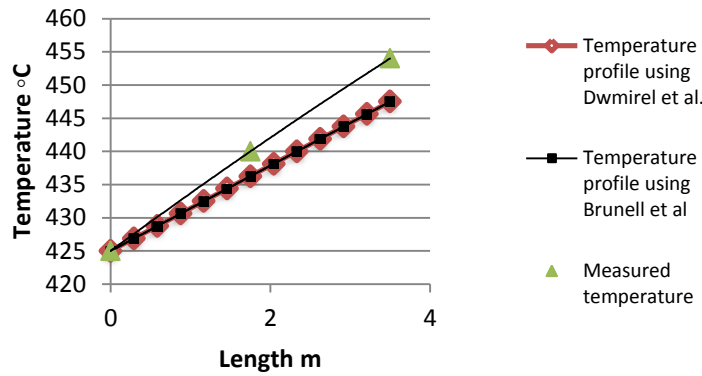


**Fig.4. Temperature profile in the axial direction using different correlations for calculating effective thermal conductivity,  $\lambda_{er}$ .**

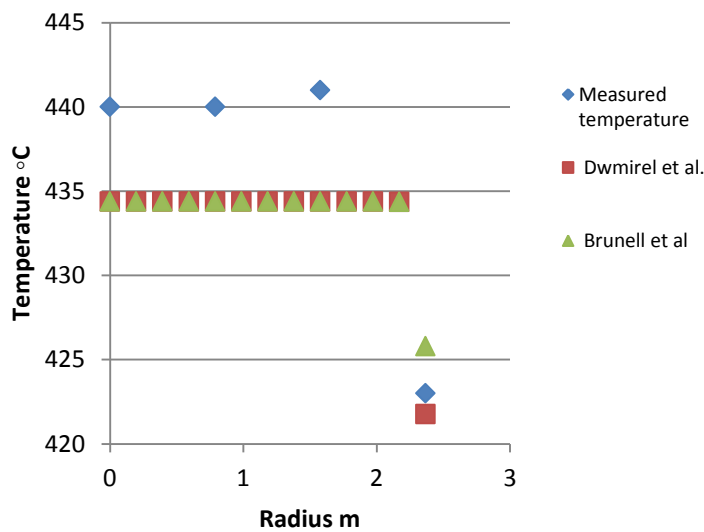


**Fig.5. Temperature profile in the radial direction using different correlations for calculating effective thermal conductivity,  $\lambda_{er}$ .**

The importance of the effective thermal conductivity rise in the radial temperature profile, where increasing its value leads to a steeper curve near the wall where temperatures are expected to decrease towards the wall of the reactor.

### 3.3. Effect of wall heat transfer coefficient ( $h_w$ ) on temperature profile

Several correlations were studied such as Wijngaarden and Westerterp [28], Borman et al. [28], Dixon and Cresswell [26], Tobis and Ziolkowski [29], Hahn and Achenbach [29]; to evaluate the wall heat transfer coefficient, and it was found that all of them gave the same good results in the axial direction as shown

in Fig.6. On the other hand, the effect of the wall heat transfer coefficient on the temperature profile in the radial direction was presented by Figs.7 and 8.

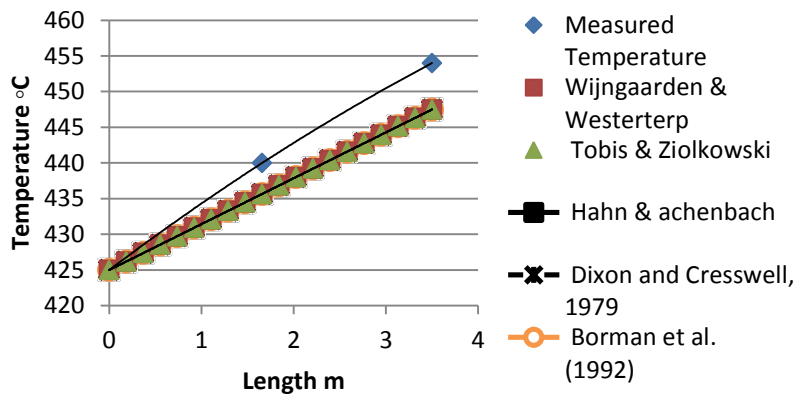


Fig. 6. Temperature profile in the axial direction using different correlations for calculating wall heat transfer coefficient,  $h_w$ .

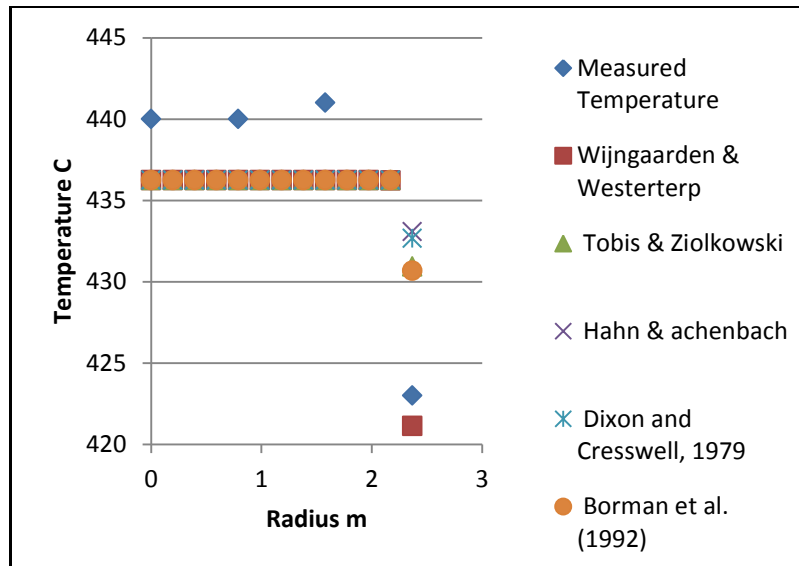
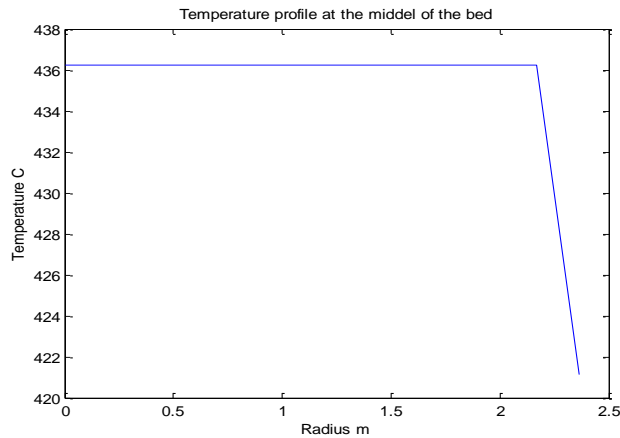


Fig. 7. Simulated and measured temperature profile in the radial direction using different correlations for calculating wall heat transfer coefficient,  $h_w$ .



**Fig. 8. Simulated temperature profile in the radial direction using Wijngaarden and Westerterp correlation.**

As shown from the previous figures, the relationship of *Wijngaarden and Westerterp* [28] shown in table 5, gave the closest temperature profile in the radial direction as it gave the lowest value of the wall heat transfer coefficient which results in a low rate of heat transferred so low wall temperature value and vice versa.

**Table 5. Experimental correlations for the wall heat transfer coefficient**

Authors	wall heat transfer coefficient	Experimental conditions
<b>Wijngaarden and Westerterp[28]</b>	$Bi_{w,p} = 2.9Nu_p^{-0.4}$	-
<b>Borman et al. [28]</b>	$Nu_w = 2.29Re_p^{0.41}$	valid for $150 < Re_p < 2000$
<b>Dixon and Cresswell[28]</b>	$Bi_{w,p}(d_p / R_t) = 3.0Re_p^{-0.25}$	valid for $Re_p > 40$
<b>Tobis and Ziolkowski[29]</b>	$\alpha_{w,f} = 0.18\lambda_f / D_p [Re/(1 - \epsilon_1)]^{0.8} Pr^{0.33}$	-
<b>Hahn and Achenbach[30]</b>	$Nu_w = (1 - \frac{1}{D/d})Re^{0.61} Pr^{1/3}$	valid for $50 < Re_p < 2 \times 10^4$

Fig. 8 shows the simulated temperature profile in the radial using *Wijngaarden and Westerterp* correlation. As shown from the previous figures that both the conversion and temperature profiles in the radial direction do not have high deviation.

**3.4. Effect of effective radial diffusivity ( $D_{er}$ ) on concentration profile**

Many correlations such as Rase equation [31], Specchia et al. (1980) [31], Froment and Hofmann (1987) [28]; were tested for the calculation of the effective diffusivity; only three correlations gave suitable values for the effective radial diffusivity. The conversion profiles in the axial direction were the same as shown in Fig. 9, However, there was a slight deviation in the radial dimension as shown in Fig. 10 because the concentrations were expected to decrease towards the centre of the bed when the diffusion limitations are significant. Although it can be seen from the results that all of them gave almost the same conversion profile; however the Rase equation [31] shown in table 6, gave the closest results when simulating the whole reactor.

**Table 6. Experimental correlations for the effective radial diffusivity ( $D_{er}$ )**

Authors	Effective Radial Diffusivity (Der)
<b>Rase equation [31]</b>	<p>For <math>d_{pa}/d_t &gt; 0.1</math> <math display="block">\frac{\varepsilon D_{er}}{u_s d_{pa}} = \frac{1}{m} + \frac{0.38}{Re}</math></p> <p>For <math>d_{pa}/d_t &lt; 0.1</math> divide <math>D_{er}</math> calculated from above by <math>\left[1 + 19.4 \left(\frac{d_{pa}}{d_t}\right)^2\right]</math></p> <p><math>m = \begin{cases} 11 &amp; Re &gt; 400 \\ 57.85 - 35.36 \log Re + 6.68 (\log Re)^2 &amp; 20 &lt; Re &lt; 400 \end{cases}</math></p>
<b>Specchia et al. [31]</b>	$D_{er} = \frac{u_s d_{pa}}{8.65 \left[1 + 19.4 \left(\frac{d_{pa}}{d_t}\right)^2\right]}$
<b>Froment and Hofmann [28]</b>	$D_{er} = \frac{d_p v_{z,s}}{10 \left[1 + 19.4 \left(\frac{d_p}{d_t}\right)^2\right]}$

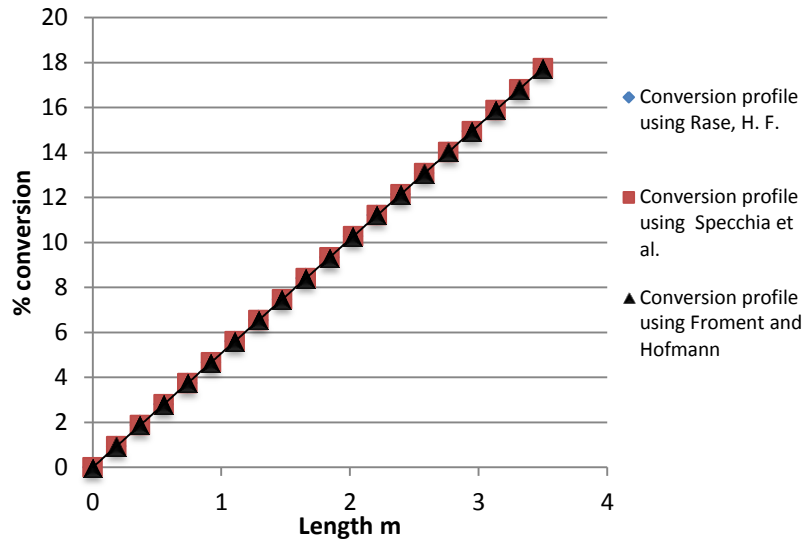


Fig. 9. Simulated percentage conversion in the axial dimension using different correlations for effective radial diffusivity.

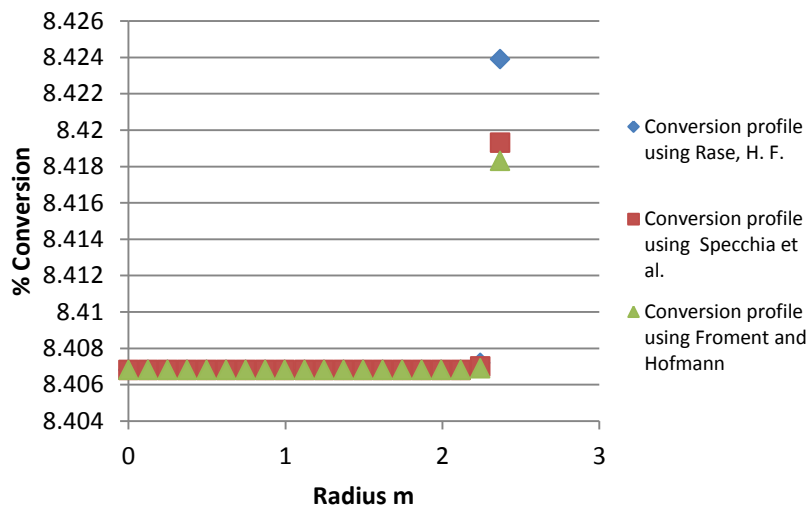


Fig. 10. Simulated percentage conversion in the radial dimension using different correlations for effective radial diffusivity.

### 3.5. Effect of cooling medium (quench zone) on conversion

Figs. 11 and 12 show the effect of quench zone on conversion for the first reactor and the second reactor respectively. As shown from the figures, the conversion increases slightly in the quench zone for both reactors despite the absence of a catalyst. The results can be explained by two points: Hydrogen addition in this part of the reactor may lead to increase the reaction rate that increases the conversion. The main aim of the quench zone is to reduce the temperature and because the reaction is exothermic conversion at equilibrium is higher.

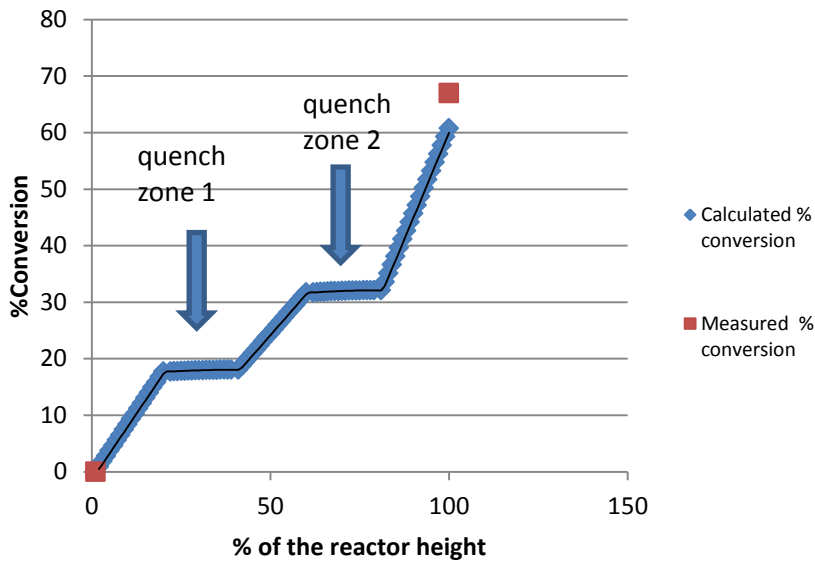


Fig. 11. Actual and simulated percentage conversion for quench zone in the radial dimension for first reactor.

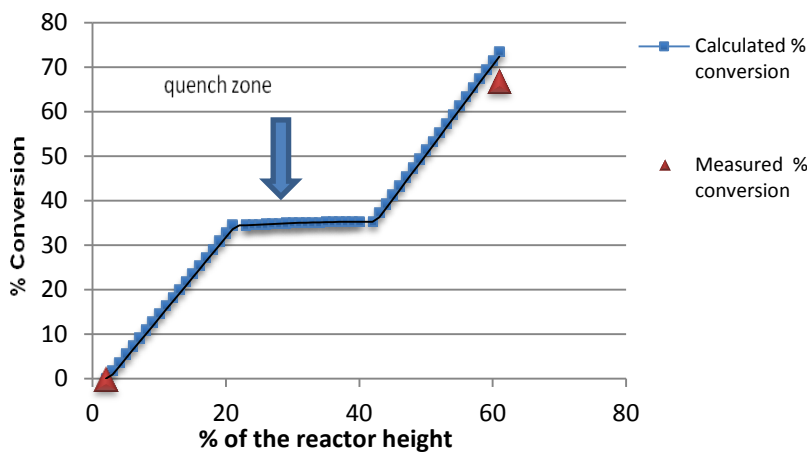


Fig. 12. Actual and simulated percentage conversion for quench zone in the radial dimension for second reactor.

#### 4. Conclusions

A rigorous two-dimensional model, including conservation equations of mass and energy was developed for simulating the operation of a hydrocracking Unit. Both the catalyst bed and quench zone have been included in this integrated model. The model is capable of predicting temperature and concentration profiles inside hydrocracking unit in both radial and axial directions. Simulation results have

been tested against available data from an actual plant. A comparison between the calculated and available data shows that this two dimensional model can represent the unit actual data very well. The following conclusions have been withdrawn:

- For concentration profiles, the percentage deviation in the first reactor was found to be 9.28% and 9.6% for the second reactor.
- A Maximum deviation of 2.4% was found in temperature profiles.
- In the quench zone the percent deviation in temperature was found to be 0.76%.
- Wakao et al. Correlation shown in Table 3, for evaluating Pellet heat Transfer Coefficient ( $h_p$ ) predicts the reactor temperature profile with a higher accuracy than Handley and Heggs Correlation.
- Correlations of Brunell et al. and Dwmirel et al. shown in Table 4. gave a suitable value for the effective thermal conductivity.
- Correlation of Wijngaarden and Westerterp shown in Table 5, for evaluating the wall heat transfer coefficient gave the closest temperature profile in the radial direction as it gave the lowest value of the wall heat transfer coefficient which results in low temperature value.
- Rase equation shown in Table 6, for the calculation of the effective diffusivity gave the closest results when considering the whole reactor.

## References

1. Kumar, A.; and Sinha, S. ( 2012). Steady state modelling and simulation of hydrocracking reactor. *Petroleum & Coal*, 54(1); 59-64.
2. Parkash,S.(2003). *Refining process handbook*. USA, Elsevier.
3. Hsu, C.S.; and Robinson P.R. (2006). *Practical advances in petroleum processing*. Volume 1, USA, Springer Science.
4. Canan, Ü.and Arkun, Y. (2012). Steady-state modelling of an industrial hydrocracking reactor by discrete lumping approach. *Proceedings of the World Congress on Engineering and Computer Science*, San Francisco, USA.
5. Meyers, R.A. (1996), *Handbook of petroleum processes*, New York, McGraw-Hill.
6. Bahmani,M.; Mohaddecy,R.S.; and Sadighi S. (2009). Pilot plant and modeling study of hydrocracking, hydrodenitrogenation and hydrodesulphurization of vacuum gas oil in a trickle bed reactor. *Petroleum & Coal*, 51 (1), 59-69.
7. Ancheyta-Juaárez, J.; Loâpez-Isunzac, F.; and Aguilar-Rodrôâguez, E. (1999). 5-Lump kinetic model for gas oil catalytic cracking. *Applied Catalysis A: General*, 177, 227-235.
8. Sadighi,S.; Ahmady,A. ; and Mohaddecy, R. S. (2010). 6-Lump kinetic model for a commercial .vacuum gas oil hydrocracker. *International Journal Of Chemical Reactor Engineering*, Volume 8.
9. Ancheyta,J.; Sánchez,S.; and Rodriguez,M.A. (2005). Kinetic modeling of hydrocracking of heavy oil fractions: a review. *Catalysis Today*, 109, 76 –92.



10. Bahmani, M.; Sadighi, S.; Mashayekhi, M. Mohaddecy, S.R.S.; and Vakili, D. (2007). Maximizing naphtha and diesel yields of an Industrial hydrocracking unit with minimal Changes. *Petroleum & Coal*, 49(1), 16-20.
11. Bhutani, N.; Ray, A. K.; and Rangaiah, G. P. (2006). Modeling, simulation, and multi-objective optimization of an industrial Hydrocracking unit. *Industrial Engineering Chemical Research*, 45, 1354 -1372.
12. Elizalde, I.; Rodríguez, M. A.; and Ancheyta, J. (2010). Modeling the effect of pressure and temperature on the hydrocracking of heavy crude oil by the continuous kinetic lumping approach. *Applied Catalysis A: General*, 382, 205 –212.
13. Alvarez, A.; Ancheyta, J.; and Muñoz, J.A.D. (2009). Modeling, simulation and analysis of heavy oil hydroprocessing in fixed-bed Reactors employing liquid quench streams. *Applied Catalysis A: General*, 361, 1–12.
14. Alvarez, A.; and Ancheyta, J. (2008). Modeling residue hydroprocessing in a multi-fixed-bed reactor system. *Applied Catalysis A: General*, 351, 148–158.
15. Verstraete, J.J.; Le Lannic, K. ; And Guibard I. (2007). Modeling fixed-bed residue hydrotreating processes. *Chemical engineering science*, 62, 5402 – 5408.
16. Aubé, F., and Sapoundjiev, H. (2000). Mathematical model and numerical simulations of catalytic flow reversal reactors for industrial applications. *Computers and chemical engineering*, 24, 2623–2632.
17. Béttega, R.; Moreira, M. F. P.; Corrêa, R. G. Freire, J. T. (2011). Mathematical simulation of radial heat transfer in packed beds by Pseudohomogeneous modeling. *Particuology*, 9, 107 –113.
18. Jung-Hwan, P. (1995). Modeling of transient heterogeneous two-dimensional catalytic packed bed reactor. *Korean Journal of Chemical Engineering*, 12(1), 80-87.
19. Houcque, D. (2005). Introduction to matlab for engineering students.
20. Moustafa, T. M.; Abou-Elreesh, M.; and Fateen, S. K. (2007). Modeling, simulation, and optimization of the catalytic reactor for methanol oxidative dehydrogenation, *Excerpt from the Proceedings of the COMSOL Conference*, Boston, USA.
21. Grevsokott, S.; Rusten, T.; Hillestad, M.; Edwin, E.; and Olsvik, O. (2001). Modeling and simulation of a steam reforming tube with furnace, *Chemical Engineering Science*, 56, 597-603.
22. Fogler, H.S. (2006). *Elements of chemical reaction engineering* (4<sup>th</sup> ed.). USA, Pearson Education, Inc.
23. Giavarini, C.; and Trifirò, F. (2006). *Encyclopaedia of hydrocarbons: refining and petrochemicals* .vol (2) , Italy, Marchesi Grafiche Editoriali S.P.A.
24. Jarullah, A. T.; Mujtaba, I.M.; and Wood, A.S. (2011). Kinetic parameter estimation and simulation of trickle-bed reactor for hydrodesulfurization of crude oil. *Chemical Engineering Science*, 66, 859 – 871.
25. Ghaj J. (2005). Non-boiling heat transfer in gas- liquid flow in pipes. *Journal of the Brazilian Society of Mechanical Science & Engineering*, Vol. XXVII, 1.
26. Nield, D.A.; and Bejan, A.(2013). *Convection in porous media*. (4<sup>th</sup> ed.). New York.

27. Wen, D.; and Ding, Y. (2006). Heat transfer of gas flow through a packed bed, *Chemical Engineering Science*, 61, 3532 - 3542.
28. Wesenberg, M.H. (2006). Gas heated steam reformer modeling. Ph.D thesis, 13-57.
29. Legawlec, B. ; and Ziolkowski, D.( 1995). Mathematical simulation of heat transfer withen tubler flow apperatus with packed bed by a model considering system inhomogenity. *Chemical Engineering Science*, Vol. 50, 4, 673- 683.
30. Achenbach, E. (1994). Heat and flow characteristics of packed beds. Institute of energy process engineering, Germany.
31. Iordanidis, A.A. (2002). Mathematical modeling of catalytic fixed bed reactors. Ph.D Thesis, 19-54.